8th Venice International School
on Lasers in Materials Science (SLIMS)
July 14-20, 2024, Isola di San Servolo,
Venice, Italy

Modeling of laser-matter interaction: Linking theory and experiment

Nadezhda M. Bulgakova

HiLASE Centre, Institute of Physics of CAS, Dolní Břežany, Czech Republic

E-mail: bulgakova@fzu.cz

SENDISO

Co-funded by the European Union

MINISTRY OF EDUCATION, YOUTH AND SPORTS

hilase

FZÚ

HiLASE Centre if the Institute of Physics of the Czech Academy of Sciences

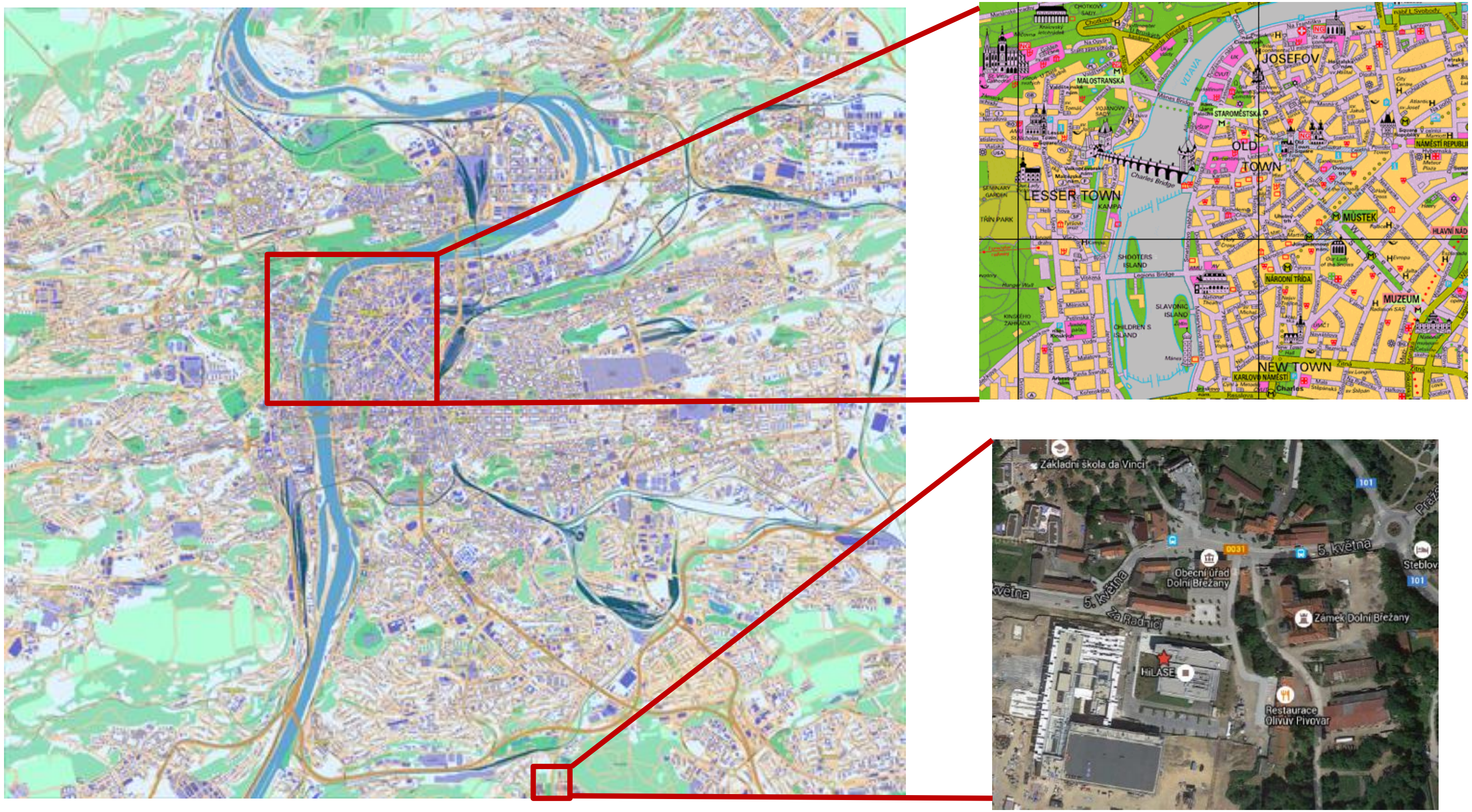

HiLASE Centre if the Institute of Physics of the Czech Academy of Sciences

Scientific Laser Applications laboratory

Pharos Laser
from Light Conversion
250 fs, 1030 nm,
200 kHz, 6W
2nd, 3rd and 4th
harmonics

Astrella Laser
from Coherent
35 fs, 800 nm, 1 kHz, 7W
2nd and 3rd harmonics

Topas OPA
from Light Conversion
for Astrella laser
50-100 fs, 1.15-15 μm

Nanosecond Lasers:
Nd:YAG with 2nd and 3rd harmonics
ArF, 193 nm

High-vacuum chamber with
Time-Of-Flight
Mass Spectrometer

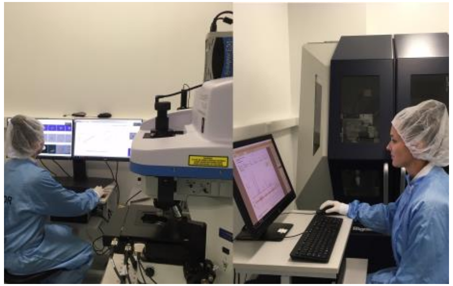

HiLASE laser (PERLA-C)
2 ps, 1030 nm, 10 kHz, 50W

Spectrometers

Hamamatsu Streak camera
1-2 ps time resolution

ICCD Camera
< 2 ns time resolution

Material characterization lab L4
AFM + Raman;
XRD; SEM

Scientific Laser Applications laboratory

Pharos Laser
from Light Conversion
250 fs, 1030 nm,
200 kHz, 6W
2nd, 3rd and 4th
harmonics

Astrella Laser
from Coherent
35 fs, 800 nm, 1 kHz, 7W
2nd and 3rd harmonics

Topas OPA
from Light Conversion
for Astrella laser
50-100 fs, 1.15-15 μm

Nanosecond Lasers:
Nd:YAG with 2nd and 3rd harmonics
ArF, 193 nm

High-vacuum chamber with Time-Of-Flight Mass

Theory is in the heart

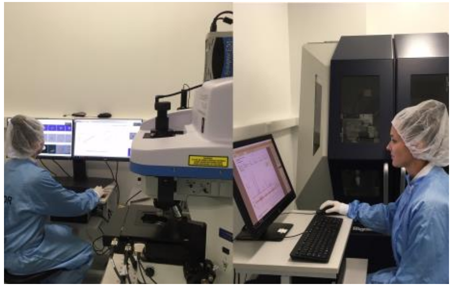

HiLASE laser (PERLA-C)
2 ps, 1030 nm, 10 kHz, 50W

Spectrometers

Hamamatsu Streak camera
1-2 ps time resolution

ICCD Camera
< 2 ns time resolution

Material characterization lab L4
AFM + Raman;
XRD; SEM

Motivation

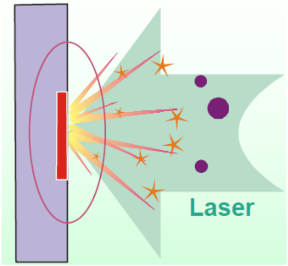

Irradiation of transparent

materials with powerful laser beams

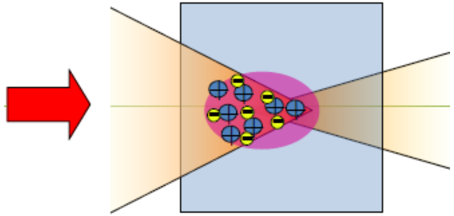

Two opposite research aims:

(1) To avoid damage: unwanted modification/cracking/defects in optics

(2) To increase energy coupling into a localized volume for achieving extreme states of matter; searching new polymorphs that possibly exhibit novel properties

A large field in between: how to gently modify material properties for laser direct writing of photonic structures which would enable light manipulations.

As a whole, the main aims of research are to learn how laser energy can be coupled in materials in the most efficient way; to predict and control the damage on the desired level, at a smallest volume; and/or to reach the highest possible stress level

Lasers in Material science

Many fascinating but still unclear phenomena

Trends

- State-of-art lasers with new radiation parameters
- Great variety of materials with very different properties
- Novel (“designed”) materials
- Flexibility in irradiation conditions: vacuum/air/inert or reactive gases or liquids; mixed targets or simultaneous/alternating action of few laser beams on several targets

Q1. What is needed for developing successful applications

CONTROL over laser-induced processes in materials is of prime importance
(INDUCED BY DIFFERENT LASERS IN DIFFERENT MATERIALS)

Processes in the pulsed laser excitation/ablation

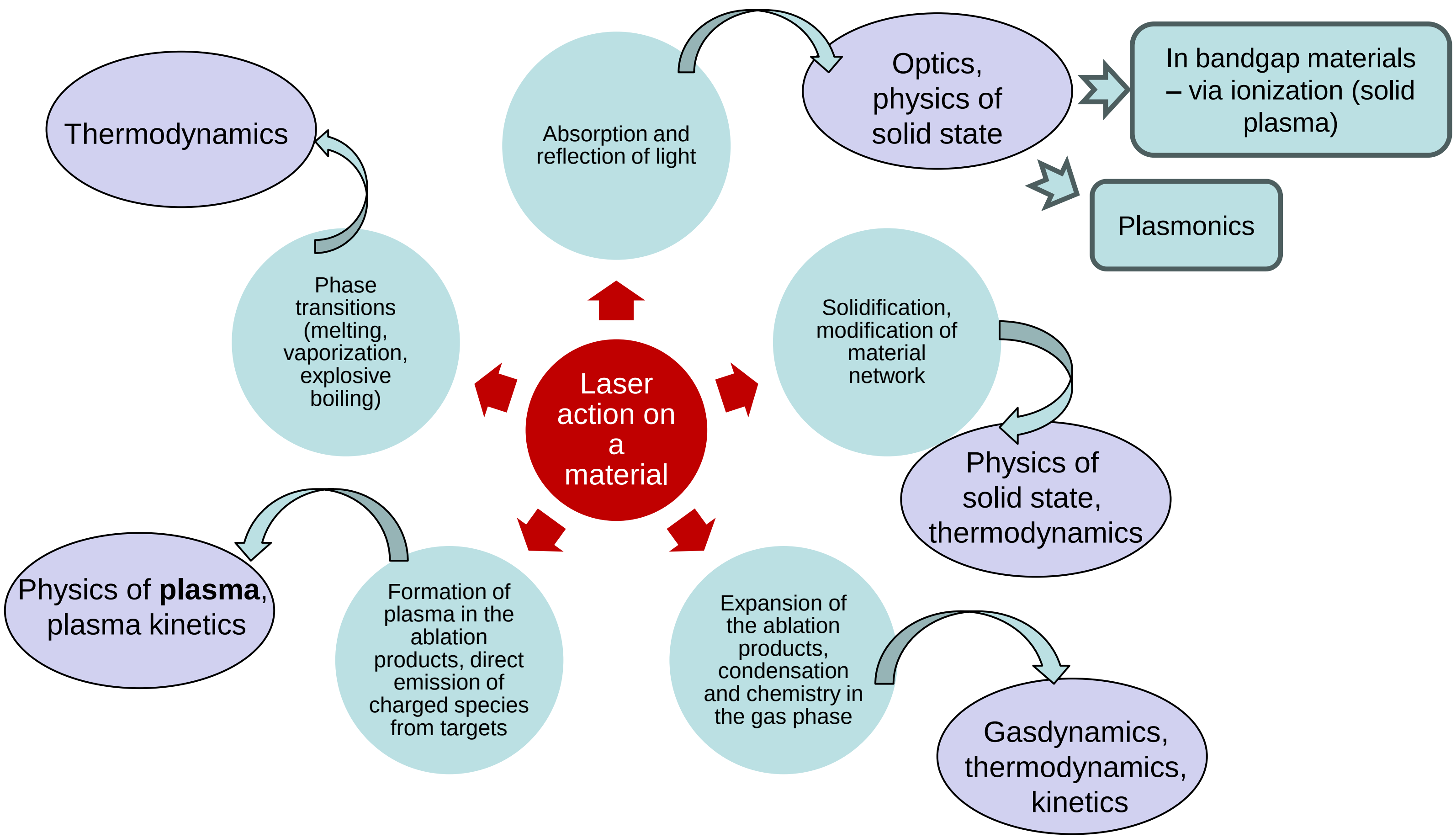

How to understand which processes are behind a phenomenon observed?

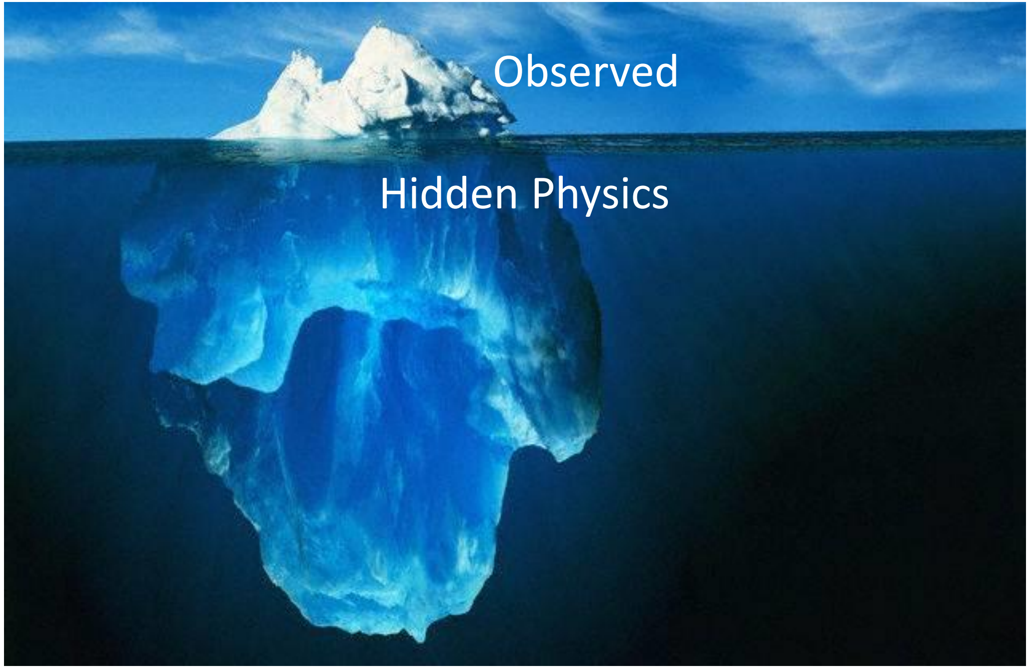

Often, in science, the real answer is usually far from obvious. Discoveries are often done when scientists ask themselves “why did this happen?” or “why isn’t this the result I expected?”

How to understand which processes are behind a phenomenon observed

Richard Phillips Feynman

Observation → We try to guess → Calculate consequences of the guess →

→ Experimental verification to check if our hypothesis/theory/modeling results are working

If the hypothesis contradicts to experiment, IT IS WRONG

IT IS NOT IMPORTANT:

How beautiful is our guess or hypothesis

How clever is the author of hypothesis

What is the name of the author

If the suggestion is not in agreement with experiment, it is false

Another problem, met not so rarely, is inaccurate modeling!

Mechanisms of nanosecond laser ablation

Laser light is absorbed by electrons

Electron-lattice thermalization time $\tau_{e\text{-}l}$ ~ 1-100 ps

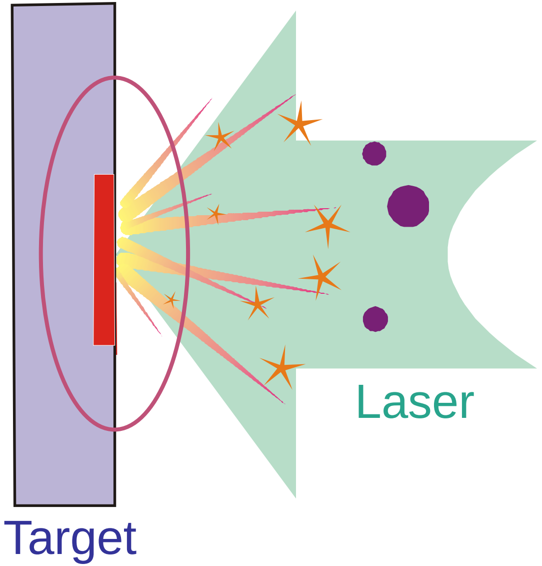

(1) Heating, (2) melting, (3) thermal vaporization

(4) phase explosion

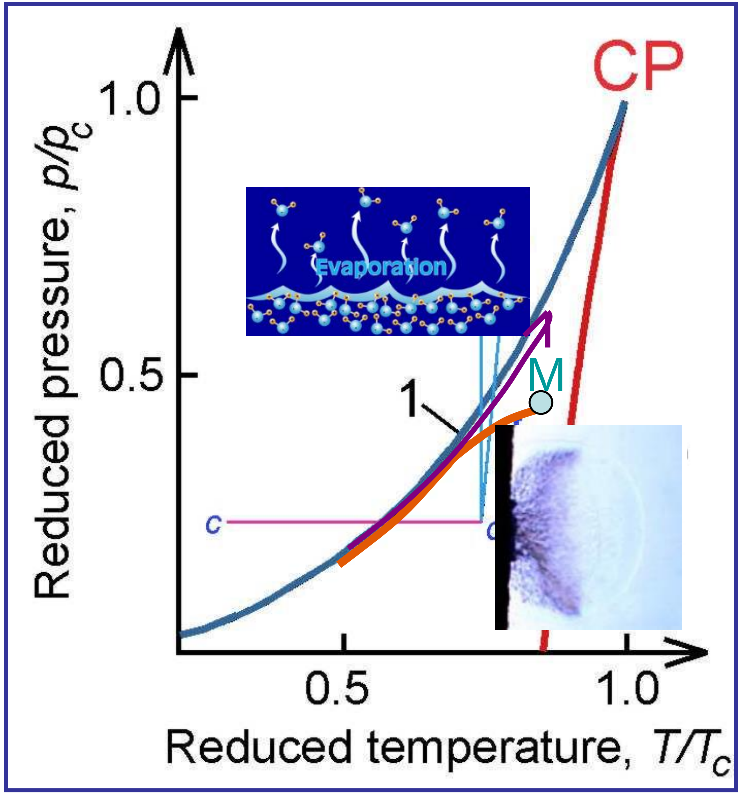

Recoil pressure → Hydrodynamic instabilities →

Mechanisms of femtosecond laser ablation

Electron-lattice thermalization time ~ 1-100 ps

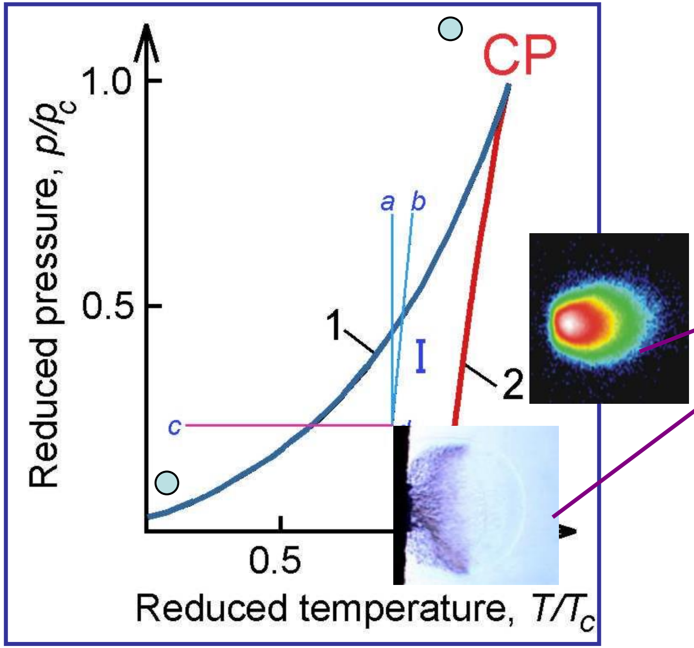

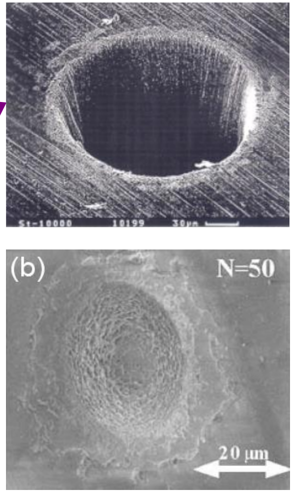

Near-ablation-threshold fluences: Spallation

Lecture by
Professor Zhigilei

Thermal processes at laser fluences typical for material processing as a function of pulse duration

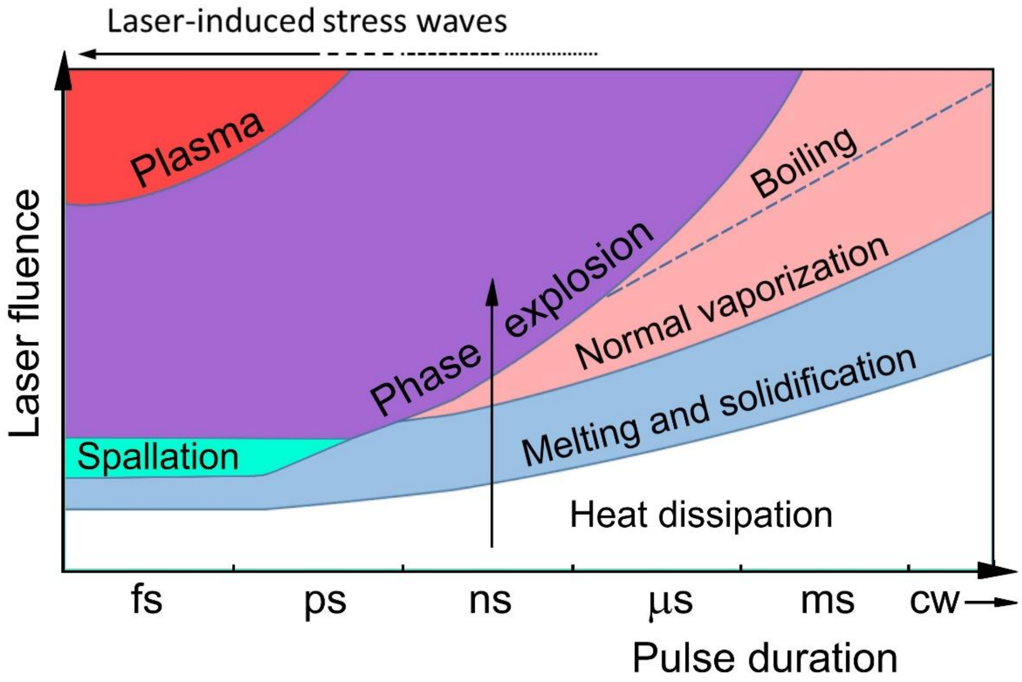

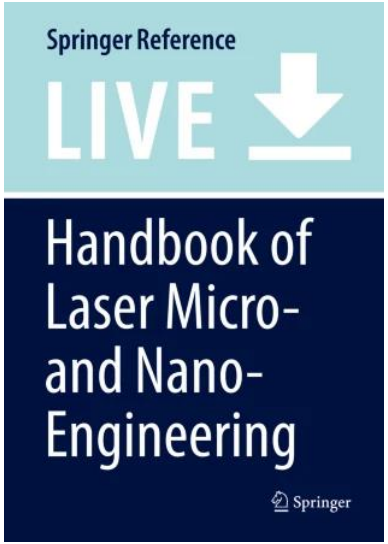

M.V. Shugaev et al. Laser-Induced Thermal Processes: Heat Transfer, Generation of Stresses, Melting and Solidification, Vaporization, and Phase Explosion, In: *Handbook of Laser Micro- and Nano-Engineering*, K. Sugioka (ed.), Springer, Cham. (2021)

Thermal processes at laser fluences typical for material processing as a function of pulse duration: long pulse durations

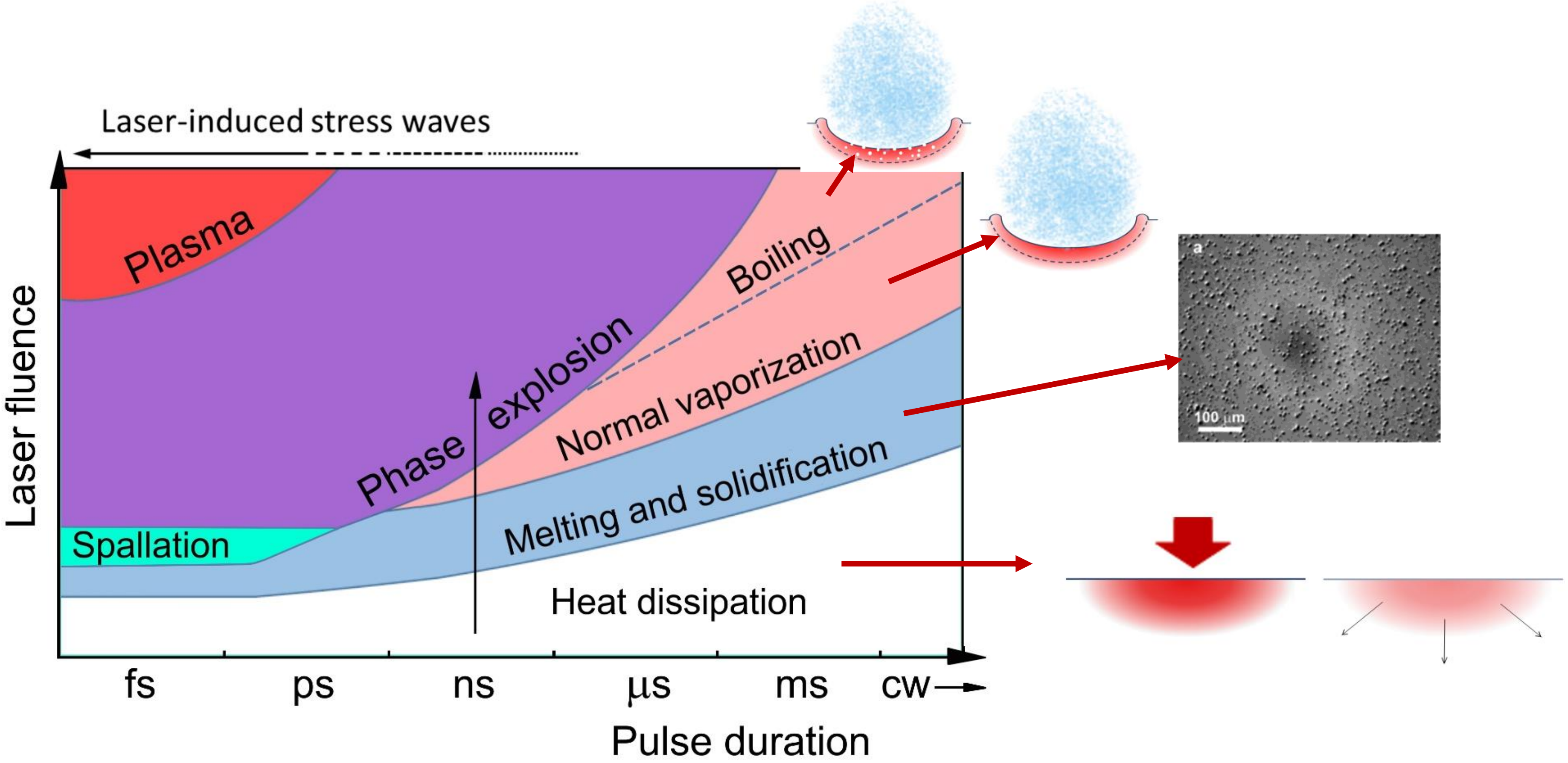

Thermal processes at laser fluences typical for material processing as a function of pulse duration: ns pulse durations

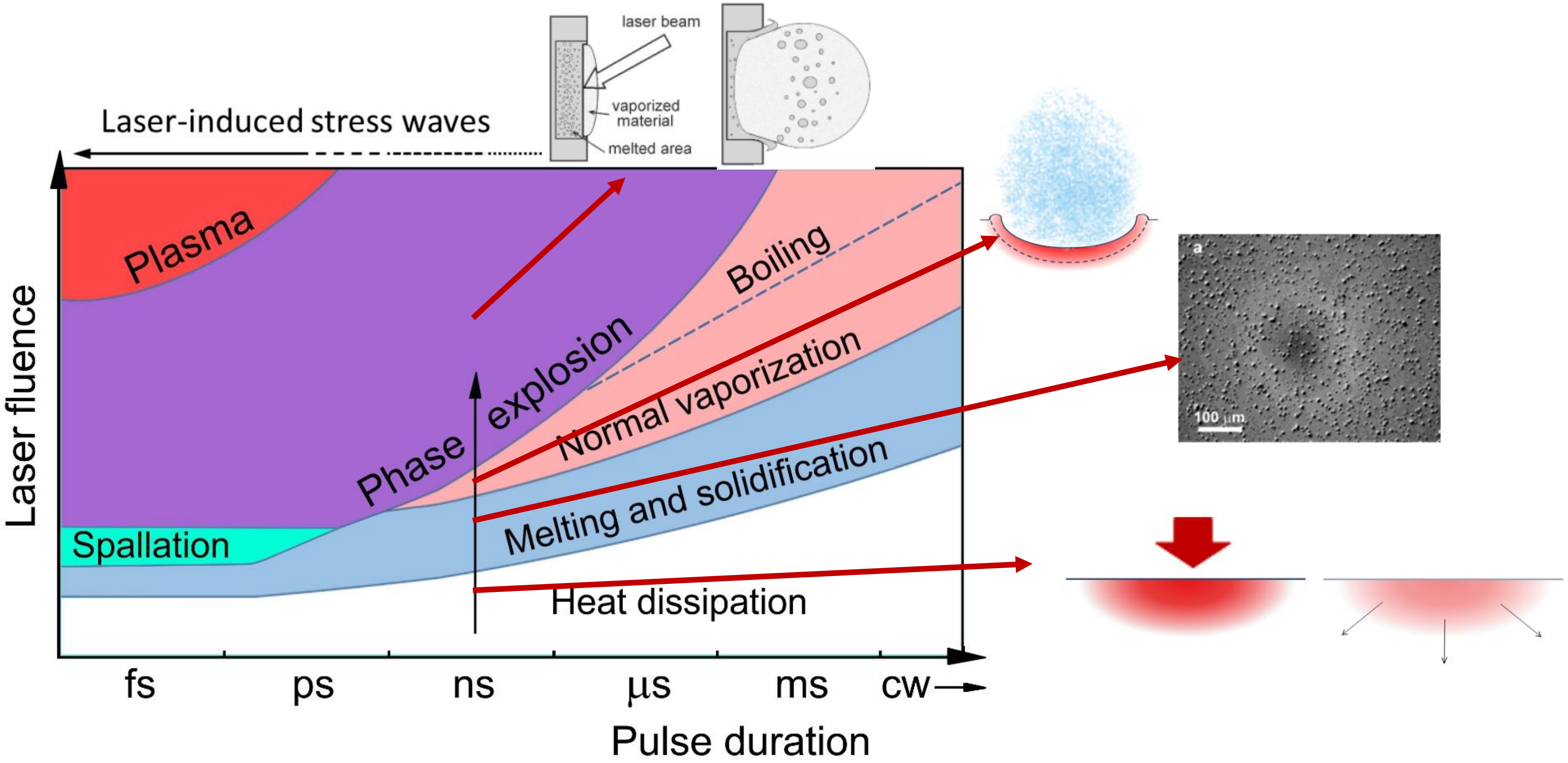

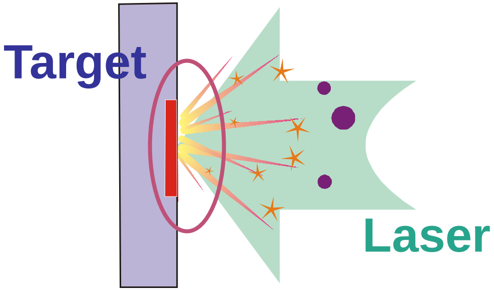

Scales of laser-affected regions:

- spot size ~10 µm – 1 mm;
- depth ~10 nm - few µm

(depending on laser focusing and absorption properties of irradiated material)

Modeling

Continuum

Density, thermal capacity, thermal conductivity, viscosity, mechanical properties (Young modulus, plastic yield, tensile strength), etc.

Mesoscopic

Combines features of macroscopic and atomistic approaches

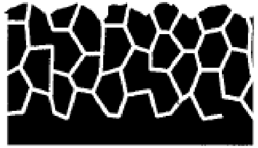

Stoneham et al.
APA 69, S81 (1999)

Atomistic

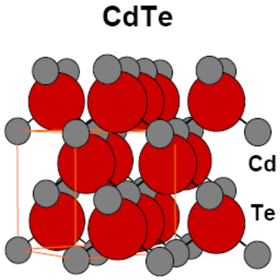

Interatomic potential of interaction

Thermal models

Pulse duration > $\tau_{e\text{-}l}$

- Heat transfer (one-temperature) model

$$C_l \frac{\partial T_l}{\partial t} = \frac{\partial}{\partial z} K_l \frac{\partial T_l}{\partial z} + \alpha(1-R) I_0(t) \exp(-\alpha z)$$

Pulse duration < $\tau_{e\text{-}l}$

- Two-temperature model

  Kaganov et al. Sov. Phys. JETP 4, 173 (1957)

$$\frac{\partial T_l}{\partial t} = \frac{T_e - T_l}{t_r}.$$

Anisimov et al. Sov. Phys. JETP 39, 375 (1974)

$$C_e \frac{\partial T_e}{\partial t} = \frac{\partial}{\partial z} K_e \frac{\partial T_e}{\partial z} - g(T_e - T_l) + \alpha(1-R) I_0(t) \exp(-\alpha z),$$

$$C_l \frac{\partial T_l}{\partial t} = \frac{\partial}{\partial z} K_l \frac{\partial T_l}{\partial z} + g(T_e - T_l)$$

Continuum modeling

- Thermal models: based of one- and two-temperature heat flow equations
- Thermal models supplemented with the equations of thermoelasticity

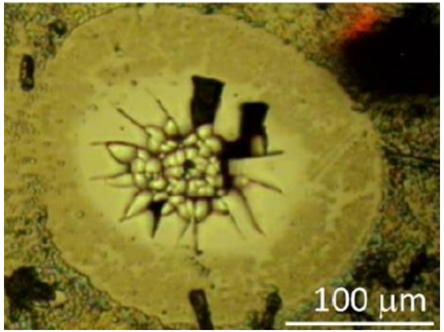

- Thermal models supplemented with the Poisson equation: laser-induced material charging
- Hydrodynamic models

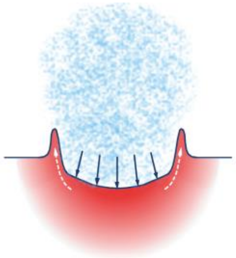

- Models based on Maxwell's equation (description of light propagation through transparent materials in the regimes of volumetric modification)

Free-electron generation and relaxation upon ultrashort laser pulse action

$$\frac{\partial n_e}{\partial t} = \sigma_n I^n + \alpha_{av} n_e I - \frac{n_e}{\tau_{tr}}$$

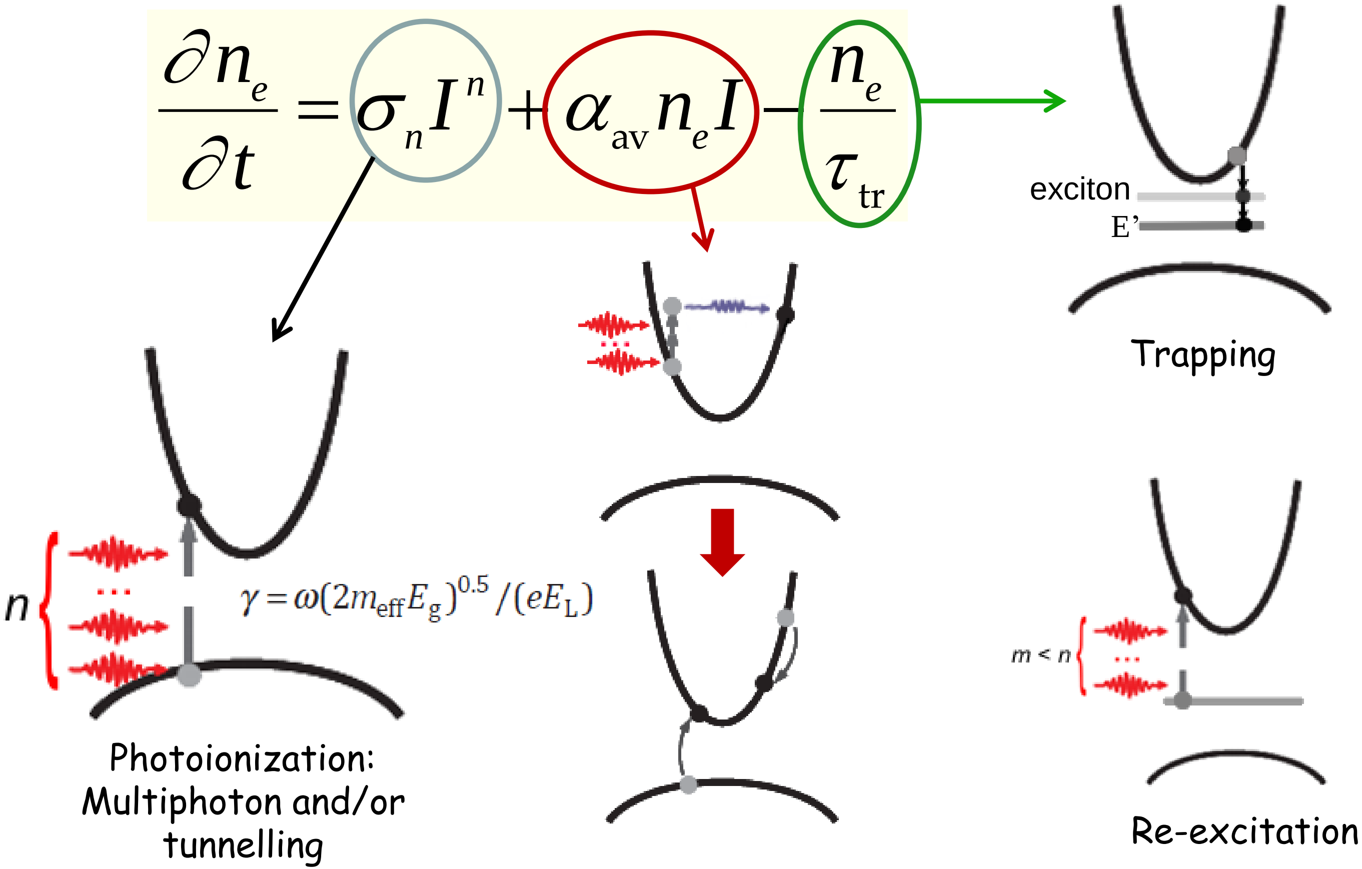

Example: Silicon excitation at 1030 nm

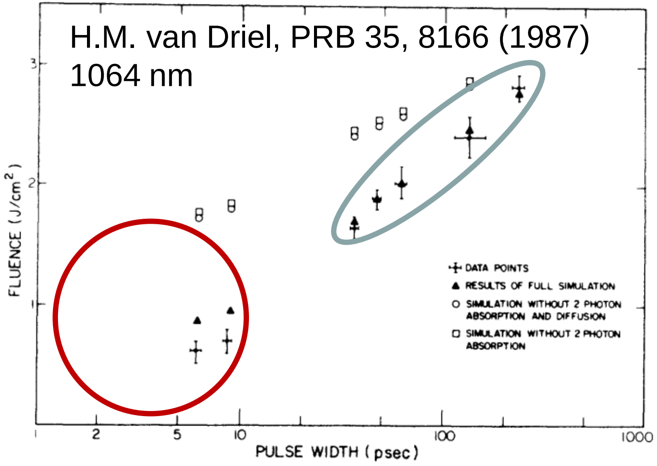

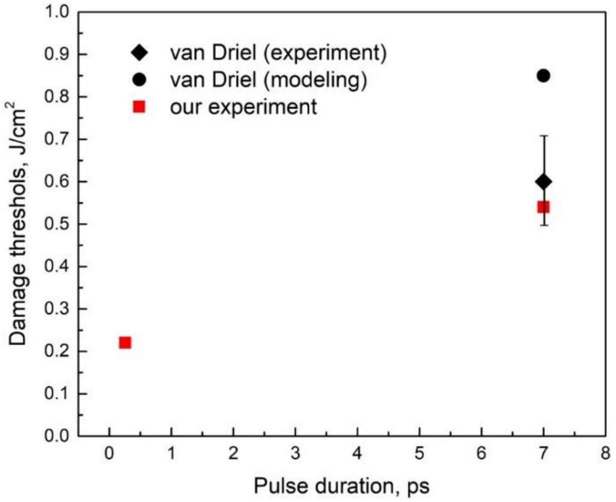

For silicon many years ago, we developed a model based on drift-diffusion approach which was largely based on van Driel model PRB 35, 8166 (1987) and partially on the paper by Sokolowski-Tinten and von der Linde, PRB 61, 2643 (2000). See, e.g., Bulgakova et al. PRB 69, 054102 (2004); APA 81, 345 (2005). All our simulations were performed for 800 nm wavelength.

Recently we applied this model for 1030 nm, our targeted wavelength. But the general aim was to verify the model and make it capable for description of ultrafast laser modification of semiconductors in a wide range of irradiation conditions.

Example: Silicon excitation at 1030 nm

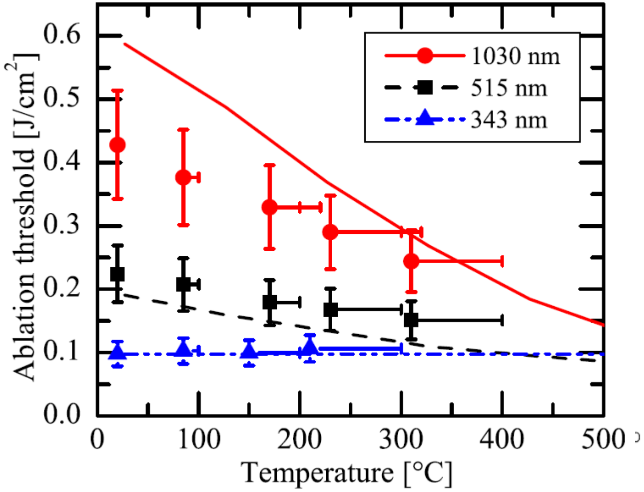

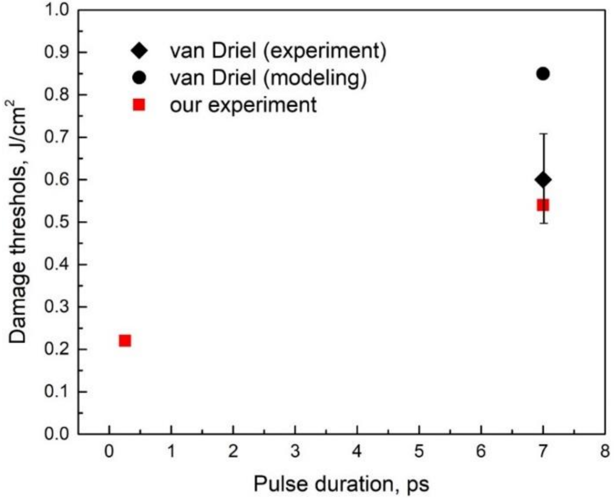

J. Thorstensen and S. E. Foss J. Appl. Phys. **112**, 103514 (2012)

For silicon many years ago, we developed a model based on drift-diffusion approach which was largely based on van Driel model PRB 35, 8166 (1987) and partially on the paper by Sokolowski-Tinten and von der Linde, PRB 61, 2643 (2000). See, e.g., Bulgakova et al. PRB 69, 054102 (2004); APA 81, 345 (2005). All our simulations were performed for 800 nm wavelength.

Recently we applied this model for 1030 nm, our targeted wavelength. But the general aim was to verify the model and make it capable for description of ultrafast laser modification of semiconductors in a wide range of irradiation conditions.

Main equations applied for silicon

Laser pulse

$$I(t) = (1 - R(t)) \frac{2F_0}{\tau_L} \sqrt{\frac{\ln 2}{\pi}} \exp\left(-4\ln 2 \left(\frac{t}{\tau_L}\right)^2\right)$$

Attenuation in the bulk

$$\frac{\partial}{\partial x} I(x,t) = -(W_1 n_a \hbar\omega + 2W_2 n_a \hbar\omega I(x,t) + \alpha_{ab}(x,t)) I(x,t)$$

Rate equation

$$\frac{\partial n_{e,h}}{\partial t} = W_1 I + W_2 I^2 + \delta n_e - R_{Auger}$$

Optical properties

$$\varepsilon^*(n_e) \cong 1 + (\varepsilon_g - 1)\left(1 - \frac{n_e}{n_0}\right) - \frac{n_e}{n_{cr}} \frac{1}{1 + i\frac{1}{\omega\tau}}$$

Energy balance for laser energy source

$$\frac{\partial E_f}{\partial t} = \left((\hbar\omega - E_g)\frac{\sigma_1 I}{\hbar\omega} + (2\hbar\omega - E_g)\frac{\sigma_2}{2}\frac{I^2}{\hbar\omega} - E_g \delta n_e\right)\frac{n_a}{n_a + n_i} + \alpha_{ab}(x,t) I(x,t) + E_g R_e$$

$$C_e \frac{\partial T_e}{\partial t} = \frac{\partial}{\partial z} K_e \frac{\partial T_e}{\partial z} - g(T_e - T_l) + \frac{\partial E_f}{\partial t},$$
$$C_l \frac{\partial T_l}{\partial t} = \frac{\partial}{\partial z} K_l \frac{\partial T_l}{\partial z} + g(T_e - T_l)$$

Temperatures as a measure of an average energy. In terms of enthalpy – the same results when taking care of algorithm accuracy.

Parameters needed for simulations

- Optical
  - Intrinsic absorption
  - Laser-induced
  - Plasma
- Thermophysical/kinetic
  - Lattice
    - Heat capacity
    - Thermal conductivity
    - Melting enthalpy
  - Electrons/holes
    - Heat capacity
    - Thermal conductivity
    - Diffusivity
    - Recombination
    - e-ph coupling

$$\frac{\partial}{\partial x} I(x,t) = -(W_1 n_a \hbar\omega + 2W_2 n_a \hbar\omega I(x,t) + \alpha_{ab}(x,t)) I(x,t)$$

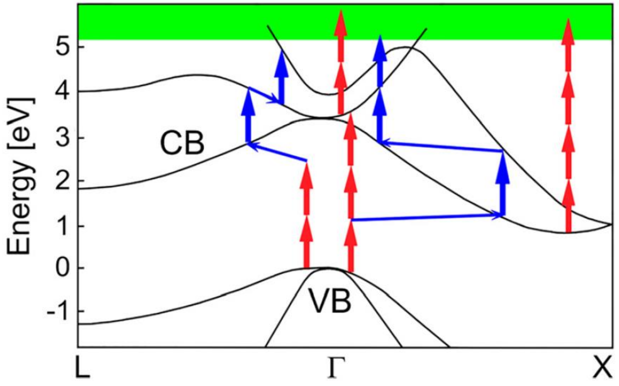

Two-photon absorption as an averaged value for photo-ionization rate (e.g. three-photon direct absorption can be efficient but its rates are not known)

Melting threshold at 1030 nm

Two-photon absorption in our modeling 7 cm/GW

$$\frac{\partial}{\partial x} I(x,t) = -(W_1 n_a \hbar\omega + 2W_2 n_a \hbar\omega I(x,t) + \alpha_{ab}(x,t)) I(x,t)$$

Thus, shortly:
In final model, we disregarded

(1) Saturation of Auger recombination at high densities of free electrons
(2) Increasing of e-ph coupling time at electron densities approaching and exceeding the critical plasma density

All other provisions are similar to previous models developed for 800 nm
Bulgakova et al. PRB 69, 054102 (2004); APA 81, 345 (2005)
Korfiatis et al. JPD 40, 6803 (2007); ASS 255, 7605 (2009)
Rämer et al. JAP 116, 053508 (2014)

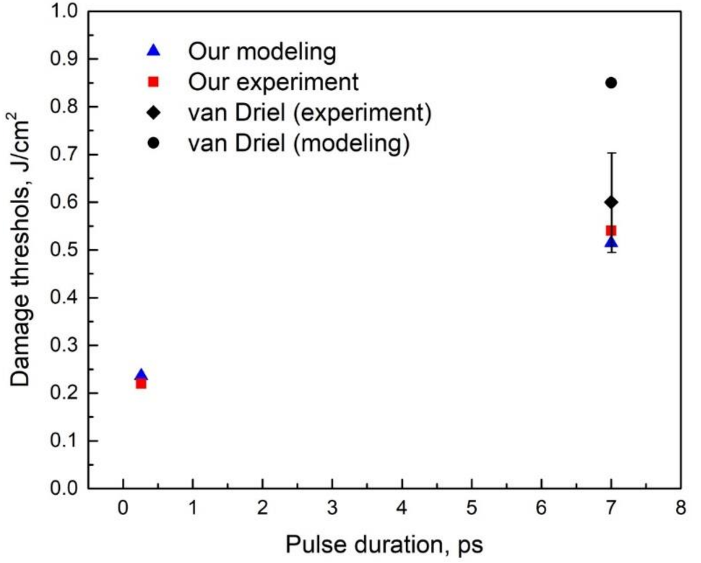

Next step:
Using **TDDFT** simulations to derive PI rates for 1030 nm and other wavelength

Time-dependent density functional theory

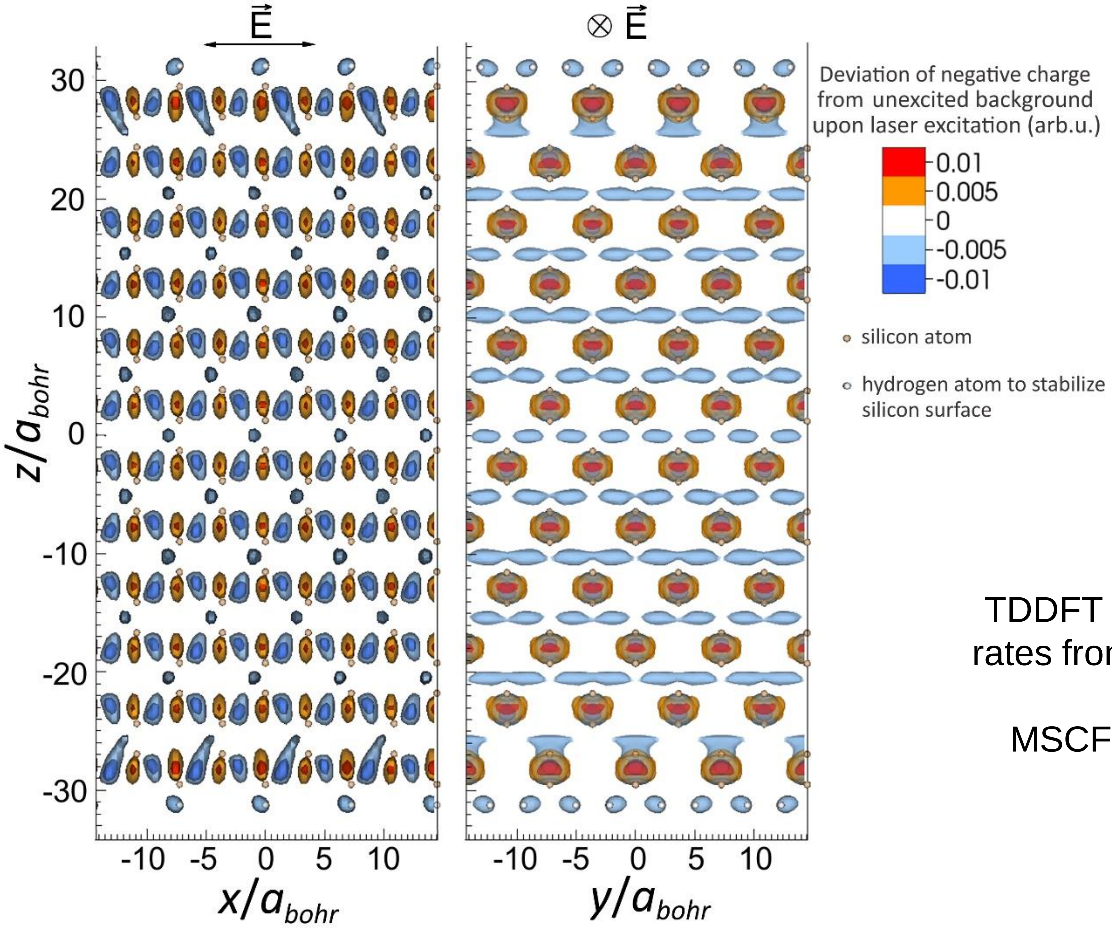

"Time-dependent density functional theory (TDDFT) can be viewed as an exact reformulation of time-dependent quantum mechanics, where the fundamental variable is no longer the many-body wave-function but the density.“
http://www.tddft.org/
I

TDDFT allows direct extraction of photoionization rates from first principles with no limitation inherent for Keldysh theory.
MSCF project (Horizon 2020): T. J.-Y. Derrien; PRB 104, L241201 (2021)

Laser annealing of multilayer structures

V.A. Volodin et al. Opt. Las. Techn. 161, 109161 (2023)

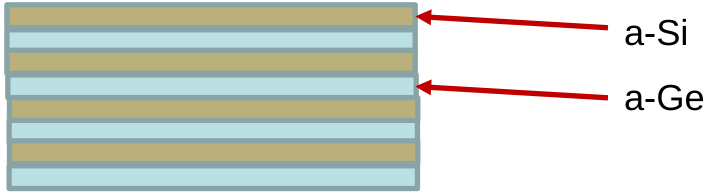

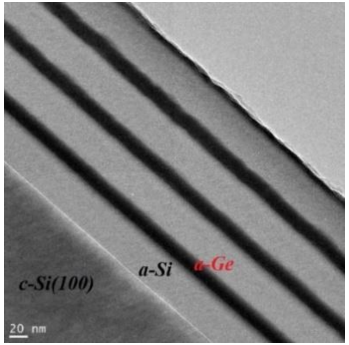

Problem to solve:

You have two lasers, 2 ps at 1030 nm and 70 fs at 1500 nm
You need to crystallize germanium to leave unaffected silicon for using in used in p-i-n photodiodes or solar cells. You have to avoid intermixing of layers.

Q2. From what to start?

(1) materials properties

For modeling, it is necessary to collect the most reliable properties of materials involved

Parameter	a-Si	a-Ge
density, ρ, g/cm^3	2.28 [Bäuerle]	5.15 [Goldschmidt]
heat capacity, c_p, J/(kg K))	800 [Bäuerle]	330 [Chen]
melting temperature, T_m, K	1420 [Bäuerle]	985 [Szyszko]
heat of fusion, ΔH_m, J/kg	$1.25 \cdot 10^6$ [Bäuerle]	$3.5 \cdot 10^5$ [Szyszko]
band gap, E_g, eV	1.7 (direct) [Shoji]	~0.45 [Goh]
one-photon absorption coefficient, α, 1/cm	0.4 at 1030 nm [Boyuan] 10^{-2} at 1500 nm [Shoji]	$3 \cdot 10^4$ at 1030 nm [Liu] $2.35 \cdot 10^3$ at 1500 nm [Liu]
two-photon absorption coefficient, β, cm/GW	2 at 1030 nm [Bristow]* 0.08 1550 nm [Shoji]	taken as negligible for 1030 nm 12 cm/GW at 1050 nm [Garcia]*
reflection coefficient, R	0.4 at 1030 nm [Palik] 0.31 at 1500 [Palik]	~0.43 at 1030 nm [Liu] ~0.4 at 1500 nm [Liu]
Young's modulus, GPa	134 GPa [Kuschnereit]	126 [Zhan]
Poisson ratio, ν	0.25 [Kuschnereit]	0.25 [Bharathan]
Linear thermal expansion coefficient, α_l, 1/K	$1 \cdot 10^{-6}$ [Takimoto]	$1.7 \cdot 10^{-5}$ (solid) [Persans] $0.9656 \cdot 10^{-4}$ (liquid) [Rhim]
Rupture tensile strength, GPA	1.6 [Brookshire]	Unknown†

Q3. What next?

(2) Laser action → photoionization (example of estimation)

$$\frac{\partial n_e}{\partial t} = \frac{(1-R)\alpha I(z,t)}{\hbar\omega} + \frac{(1-R)^2\beta I^2(z,t)}{2\hbar\omega} + \delta(T_e)n_e - Cn_e^2 n_i$$

$$n_e \sim \frac{(1-R)\alpha I\tau}{\hbar\omega} + \frac{(1-R)^2\beta I^2\tau}{2\hbar\omega} = \frac{(1-R)\alpha F}{\hbar\omega} + \frac{(1-R)^2\beta F^2}{2\hbar\omega\tau}$$

Results of estimations for 70-fs laser pulses at λ=1500 nm of the electron number densities generated in 1PA and 2PA processes, lattice temperature expected after electron-lattice thermalization, and the fraction of the molten phase *f*.

Fluence, mJ/cm^2	a-Si			a-Ge				
	n_e, cm^{-3} (1PI)	n_e, cm^{-3} (2PI)	T, K	n_e, cm^{-3} (1PI)	n_e, cm^{-3} (2PI)	T+ΔT, K	T - $f\Delta H_m$, K	f
40	$2.16\cdot10^{15}$	$3.4\cdot10^{18}$	301	$7.86\cdot10^{20}$	$3.86\cdot10^{20}$	541	541	0
55	$2.96\cdot10^{15}$	$6.43\cdot10^{18}$	302	$1.34\cdot10^{21}$	$7.3\cdot10^{20}$	710	710	0
70	$3.77\cdot10^{15}$	$1.04\cdot10^{19}$	303.4	$1.95\cdot10^{21}$	$1.18\cdot10^{21}$	896	896	0
100	$5.39\cdot10^{15}$	$2.12\cdot10^{19}$	306.7	$3.5\cdot10^{21}$	$2.4\cdot10^{21}$	1370	985	0.36
150	$8.09\cdot10^{15}$	$4.78\cdot10^{19}$	315	$7.05\cdot10^{21}$	$5.4\cdot10^{21}$	2457	1396	1
190	$1.02\cdot10^{16}$	$7.64\cdot10^{19}$	325	$1.08\cdot10^{22}$	$8.7\cdot10^{21}$	3604	2543	1

Q4. What next?

(3) Temperature and molten fraction evaluation

$$c_p \rho \Delta T = (E_g + E_{\mathrm{av}}^e)$$

$$f = c_p (T - T_m)/\Delta H_m,$$

Results of estimations for 70-fs laser pulses at λ=1500 nm of the electron number densities generated in 1PA and 2PA processes, lattice temperature expected after electron-lattice thermalization, and the fraction of the molten phase *f*.

Fluence, mJ/cm^2	a-Si			a-Ge				
	n_e, cm^{-3} (1PI)	n_e, cm^{-3} (2PI)	T, K	n_e, cm^{-3} (1PI)	n_e, cm^{-3} (2PI)	T+ΔT, K	$T - f\Delta H_m$, K	f
40	$2.16\cdot10^{15}$	$3.4\cdot10^{18}$	301	$7.86\cdot10^{20}$	$3.86\cdot10^{20}$	541	541	0
55	$2.96\cdot10^{15}$	$6.43\cdot10^{18}$	302	$1.34\cdot10^{21}$	$7.3\cdot10^{20}$	710	710	0
70	$3.77\cdot10^{15}$	$1.04\cdot10^{19}$	303.4	$1.95\cdot10^{21}$	$1.18\cdot10^{21}$	896	896	0
100	$5.39\cdot10^{15}$	$2.12\cdot10^{19}$	306.7	$3.5\cdot10^{21}$	$2.4\cdot10^{21}$	1370	985	0.36
150	$8.09\cdot10^{15}$	$4.78\cdot10^{19}$	315	$7.05\cdot10^{21}$	$5.4\cdot10^{21}$	2457	1396	1
190	$1.02\cdot10^{16}$	$7.64\cdot10^{19}$	325	$1.08\cdot10^{22}$	$8.7\cdot10^{21}$	3604	2543	1

Crystallization of Ge layer; Si layers stay intact; no any signes of intermixing between Ge and Si layers that was requested for application

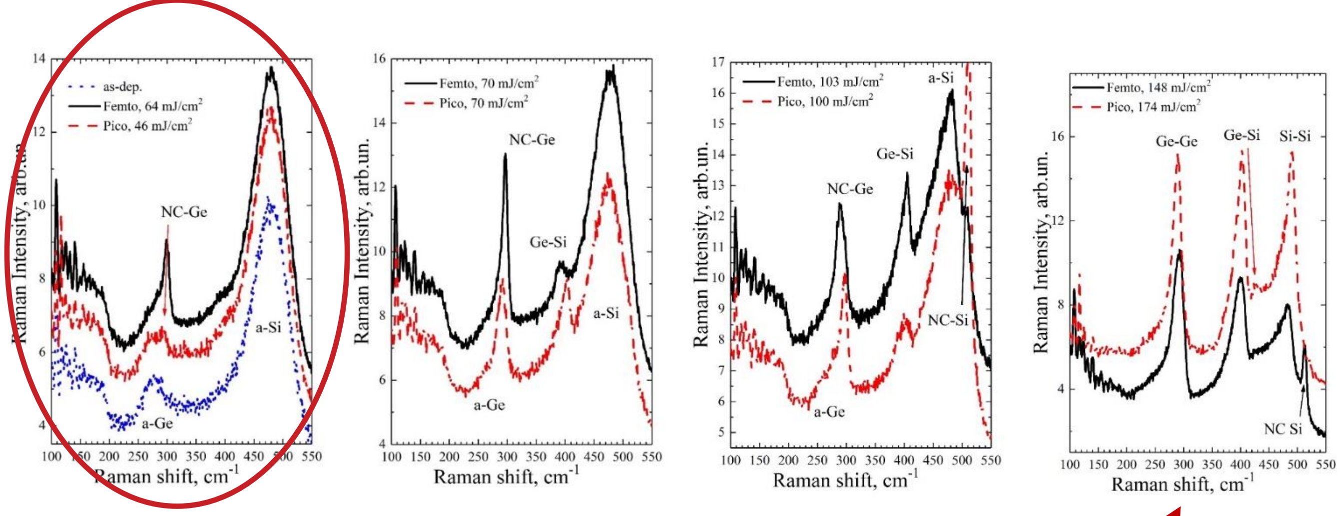

Fluence, mJ/cm^2	a-Si			a-Ge				
	n_e, cm^{-3} (1PI)	n_e, cm^{-3} (2PI)	T, K	n_e, cm^{-3} (1PI)	n_e, cm^{-3} (2PI)	T+ΔT, K	T - fΔH_m, K	f
40	$2.16\cdot10^{15}$	$3.4\cdot10^{18}$	301	$7.86\cdot10^{20}$	$3.86\cdot10^{20}$	541	541	0
55	$2.96\cdot10^{15}$	$6.43\cdot10^{18}$	302	$1.34\cdot10^{21}$	$7.3\cdot10^{20}$	710	710	0
70	$3.77\cdot10^{15}$	$1.04\cdot10^{19}$	303.4	$1.95\cdot10^{21}$	$1.18\cdot10^{21}$	896	896	0
100	$5.39\cdot10^{15}$	$2.12\cdot10^{19}$	306.7	$3.5\cdot10^{21}$	$2.4\cdot10^{21}$	1370	985	0.36
150	$8.09\cdot10^{15}$	$4.78\cdot10^{19}$	315	$7.05\cdot10^{21}$	$5.4\cdot10^{21}$	2457	1396	1
190	$1.02\cdot10^{16}$	$7.64\cdot10^{19}$	325	$1.08\cdot10^{22}$	$8.7\cdot10^{21}$	3604	2543	1

Formation of GeSi alloy

(4) Stress-induced explosive crystallization

$$\sigma_r^{max} = \frac{E\alpha_l \Delta T}{2(1-\nu)},$$

The stresses in a-Ge nanolayers upon irradiation with 1500 nm wavelength are evaluated to increase from 0.34 GPa at 40 mJ/cm^2 to 0.97 GPa at 100 mJ/cm^2

(5) *Can non-thermal melting promote a-Ge crystallization?* We note that, in fs irradiation regimes, the density of the ionized atoms in a-Ge approaches the criterium of ultrafast (non-thermal) melting (~10-15% of the valence electrons is pumped to the conduction band). Such excitation is almost immediately followed by lattice destabilization culminating innonthermal phase transitions (ultrafast melting) on a sub-ps time scale. Although ultrafast melting in *amorphous* semiconductors looks to be unobservable, lattice atoms become mobile and can form crystallites. For low-bandgap semiconductors as a-Ge, from the energy balance one can expect a situation when ultrafast melting is not followed by thermal melting.

Fluence, mJ/cm^2	**a-Si**			**a-Ge**				
	n_e, cm^{-3} (1PI)	n_e, cm^{-3} (2PI)	T, K	n_e, cm^{-3} (1PI)	n_e, cm^{-3} (2PI)	T+ΔT, K	T - fΔH_m, K	f
40	$2.16\cdot10^{15}$	$3.4\cdot10^{18}$	301	$7.86\cdot10^{20}$	$3.86\cdot10^{20}$	541	541	0
55	$2.96\cdot10^{15}$	$6.43\cdot10^{18}$	302	$1.34\cdot10^{21}$	$7.3\cdot10^{20}$	710	710	0
70	$3.77\cdot10^{15}$	$1.04\cdot10^{19}$	303.4	$1.95\cdot10^{21}$	$1.18\cdot10^{21}$	896	896	0
100	$5.39\cdot10^{15}$	$2.12\cdot10^{19}$	306.7	$3.5\cdot10^{21}$	$2.4\cdot10^{21}$	1370	985	0.36
150	$8.09\cdot10^{15}$	$4.78\cdot10^{19}$	315	$7.05\cdot10^{21}$	$5.4\cdot10^{21}$	2457	1396	1
190	$1.02\cdot10^{16}$	$7.64\cdot10^{19}$	325	$1.08\cdot10^{22}$	$8.7\cdot10^{21}$	3604	2543	1

(4) Stress-induced explosive crystallization

$$\sigma_r^{max} = \frac{E\alpha_l \Delta T}{2(1-\nu)},$$

Observation → We try to guess → Calculate consequences of the guess →

→ Experimental verification to check if our hypothesis/theory/modeling results are working

If the hypothesis contradicts to experiment, IT IS WRONG

as a-Ge, from the energy balance one can expect a situation when ultrafast melting is not followed by thermal melting.

Fluence, mJ/cm^2	a-Si			a-Ge				
	n_e, cm^{-3} (1PI)	n_e, cm^{-3} (2PI)	T, K	n_e, cm^{-3} (1PI)	n_e, cm^{-3} (2PI)	T+ΔT, K	T - fΔH_m, K	f
40	$2.16\cdot10^{15}$	$3.4\cdot10^{18}$	301	$7.86\cdot10^{20}$	$3.86\cdot10^{20}$	541	541	0
55	$2.96\cdot10^{15}$	$6.43\cdot10^{18}$	302	$1.34\cdot10^{21}$	$7.3\cdot10^{20}$	710	710	0
70	$3.77\cdot10^{15}$	$1.04\cdot10^{19}$	303.4	$1.95\cdot10^{21}$	$1.18\cdot10^{21}$	896	896	0
100	$5.39\cdot10^{15}$	$2.12\cdot10^{19}$	306.7	$3.5\cdot10^{21}$	$2.4\cdot10^{21}$	1370	985	0.36
150	$8.09\cdot10^{15}$	$4.78\cdot10^{19}$	315	$7.05\cdot10^{21}$	$5.4\cdot10^{21}$	2457	1396	1
190	$1.02\cdot10^{16}$	$7.64\cdot10^{19}$	325	$1.08\cdot10^{22}$	$8.7\cdot10^{21}$	3604	2543	1

Tasuku Honjo, an immunology and genomic medicine professor at Kyoto University (2018 Nobel Prize in Physiology or Medicine and is best known for his identification of programmed cell death protein), said his advice for people who want to pursue a career in scientific research what he called the "six Cs":

curiosity, courage, challenges, continuation, concentration and confidence.

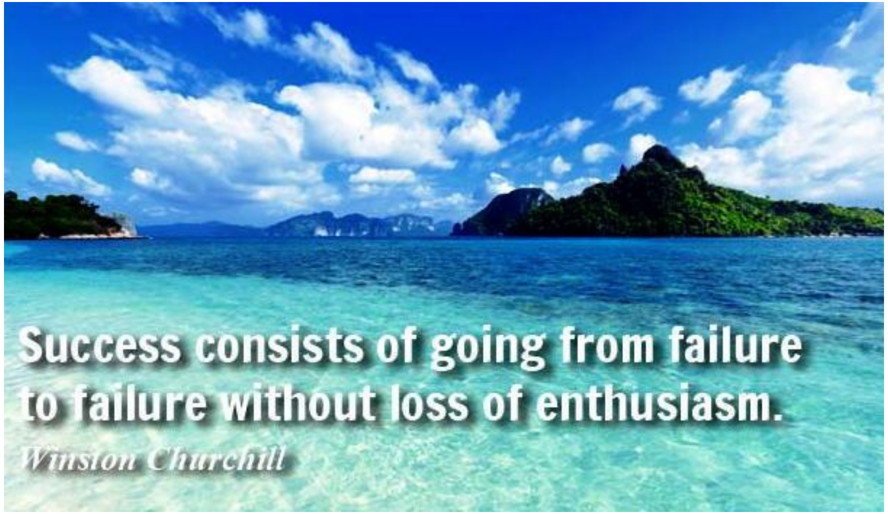

hilase
BIATRI
EVROPSKÁ UNIE
Evropské strukturální a investiční fondy
Operační program Výzkum, vývoj a vzdělávání
This project has received funding from the European Union's Horizon 2020 research and innovation programme under grant agreement No 739573 (HiLASE CoE)
FZÚ

Acknowledgements

Operational Programme Johannes Amos Comenius and financed by European Structural and Investment Funds and the Czech Ministry of Education, Youth and Sports (project SenDiSo, No. CZ.02.01.01/00/22_008/0004596)

Thank you!

SENDISO

Co-funded by the European Union

MINISTRY OF EDUCATION, YOUTH AND SPORTS

FZÚ